Environ Earth Sci (2013) 68:1609–1617
DOI 10.1007/s12665-012-1854-1

ORIGINAL ARTICLE

# Magnetic mineralogy and its implication of contemporary coastal sediments from South China

**Tingping Ouyang · Erwin Appel · Guodong Jia · Ningsheng Huang · Zhaoyu Zhu**

Received: 23 July 2011 / Accepted: 10 July 2012 / Published online: 22 July 2012


**Abstract** Magnetic parameters have been widely used as a rapid, cost-effective, and non-destructive method. To assess whether their magnetic properties reflect the development history in the Pearl River Delta, three sediment cores collected from South China coastal waters were selected for magnetic research. The results indicate that the predominant ferrimagnetic mineral is magnetite, with an additional smaller amount of surprisingly high-coercive greigite. Fine-grained superparamagnetic and single-domain particles of magnetite and the relative contribution of greigite are increased when the total concentration of ferrimagnetic minerals is higher. Three well-known stages of the Chinese history, i.e., iron smelting, cultural revolution, and the latest phase of opening and reforming were identified in the vertical variation of magnetic concentration parameters. Although the record of the three cores is not completely consistent, the results point out that magnetic concentration parameters can reflect the development and pollution history in surrounding coastal areas.

**Keywords** Magnetic mineralogy · Environmental implication · Coastal sediments · South China

T. Ouyang (✉) · G. Jia · N. Huang · Z. Zhu
Key Laboratory of Margin Sea Geology, Guangzhou Institute of Geochemistry, Chinese Academy of Sciences, Wushan, Guangzhou 510640, Guangdong, People's Republic of China
e-mail: oyangtp@gig.ac.cn

T. Ouyang · E. Appel
Department of Geosciences, University of Tübingen, Sigwartstrasse 10, 72076 Tübingen, Germany

## Introduction

Environmental magnetism has been widely used for paleoclimate reconstruction, e.g., rainfall estimation, as well as sediment provenance analyses (Evans et al. 1997; Maher 2007; Wang et al. 2009). Magnetic properties of marine sediments can often contribute reliable information on environmental change (Kumar et al. 2005; Sangode et al. 2007; Yang et al. 2008; Alagarsamy 2009; Zheng et al. 2010) and magnetic parameters such as magnetic susceptibility (MS) became a kind of basic data for marine sediment research (Evans and Heller 2003; Yim et al. 2004; Ghilardi et al. 2008; Meena et al. 2011). As a fast and cost-effective parameter, MS also has been successfully used as a proxy for the detection of anthropogenic pollution caused by metallurgical dusts, fly ashes from power plants and urban airborne particulates (Bityukova et al. 1999; Jordanova et al. 2003; Gautam et al. 2004; Lu et al. 2007). Furthermore, previous studies have shown the potential of magnetic properties for assessment of pollution in coastal areas (Plater et al. 1998; Plater and Appleby 2004; Ridgway and Shimmield 2002; Martins et al. 2007). Magnetic materials from industries and traffic are taken by water runoff or wind and then deposit in estuary and marine sediments (Locke and Bertine 1986). Therefore, magnetic signals from such deposits may be helpful to reconstruct the development or pollution history in the surrounding areas.

While numerous studies concerned the relationship between MS and the development or pollution history using sediments from lakes or man-made ponds (Hu et al. 2003; Power and Worsley 2009), the use of magnetic properties from coastal sediments for such purpose has been limited because of multiple influencing factors. Magnetic minerals and their sources must be determined

before one can relate magnetic parameters of marine sediments to the development history (Hilton 1987; Yu and Oldfield 1989). Some researches (Zhang et al. 2001; Horng and Chen 2006; Garming 2006) discussed magnetic mineral assemblages and their influencing factors for intertidal and marine sediments. However, the mechanism between magnetic properties and minerals within coastal sediments remains unclear.

In the present paper, magnetic properties of coastal sediments from the South China Sea are investigated. The surrounding area of the PRD has been experienced a specific development history since the establishment of the People's Republic of China in 1949. Hong Kong began its labor-intensive manufacturing activities and became a major exporter of clothing and toys, as well as watches and transistor radios since the early 1950s (Sung et al. 1996). Industries developed quickly in China mainland after the liberation war and establishment of the PR China, especially during the periods of the first and second 5-year-plans. Industrialization was rapidly promoted within this area, since the Central Government of China implemented its "open door" policy from late 1970s (Lo 1989; Lin 1997). The main purpose of the present study is to seek for the indication of magnetic parameters on magnetic mineralogy within these sediments, and then to discuss the feasibility of using magnetic parameters of coastal sediments to interpret the development or pollution history in the surrounding areas.

## Materials and methods

### Sample sites and dating

Core samples analysed in the present paper were collected from southern Chinese coastal waters in summer 2009, using box-type samplers. Figure 1 shows the location of the sampling sites. Cores A8 (21.8°N, 114.2°E) and A9 (22.0°N, 114.0°E) mainly reflect terrigenous input of the Pearl River (Zhang et al. 2010; Li et al. 2011). Water depths of these two sites are 45 and 33 m, respectively. Sampling site E601 (20.9°N, 112.1°E) is located at the southwest region of the Pearl River Estuary (PRE) and receives part of the terrigenous materials input from the PRE due to coastal currents (Fig. 1; Liu et al. 2010a); water depth at site E601 is 53 m. Total lengths of cores A8, A9, and E601 are 58, 54, and 40 cm, respectively. After shipping to laboratory, the cores were subsampled into individual specimens, using 2-cm spacing, and were freeze dried.

The $^{210}$Pb method was used for dating (Nittrouer et al. 1979) measurements were performed using an Ortec HPGe GEM/Lo-Ax/GMX at the Institute of Earth Sciences,

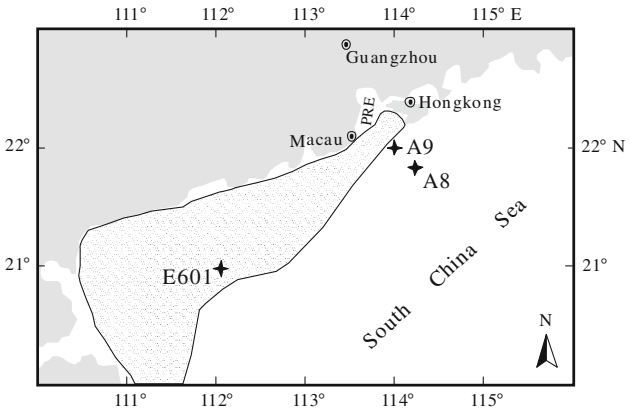


**Fig. 1** Location of sampling cores. *PRE* denotes the Pearl River Estuary; the *shaded area* represents the area within the South China Sea which receives material from the PRE due to coastal currents (modified from Liu et al. 2010a). The location of cores A8 and A9 are supplied with material by the Pearl River currents

Academia Sinica, Taiwan (Huh et al. 2006). International standard reference materials (NBS-4353, IAEA-133A, 327, 375) were used for energy, efficiency and mass calibration for every detector. Constant $^{210}$Pb activities in the lower portions of the cores are assumed to represent supported Pb, and this value was subtracted from total activity to yield excess $^{210}$Pb activity. Because each core displayed log-linear excess $^{210}$Pb profiles when plotted against cumulative mass, the constant initial concentration (CIC) model was used for age and sediment mass accumulation rate (MAR) calculation (Krishnaswami et al. 1971). Accordingly, core A8 was found to span a history from 1880 to present, core A9 from 1920 to present, and for core E601 an age of 1905 is found at depths of 28–30 cm. Details of the dating method and age calculations will be published elsewhere (Chen et al. in preparation).

### Mineral magnetic analysis

Grain size and concentration of magnetic minerals within a sample can be identified from magnetic properties. A suite of mineral magnetic analyses were performed in this study. MS along the cores and temperature variation of MS were measured at the Guangzhou Institute of Geochemistry, Chinese Academy of Sciences. All other magnetic measurements were performed at the Department for Geosciences, University of Tuebingen.

Low (976 Hz) and high (15,616 Hz) frequency susceptibility (mass-specific $\chi_{lf}$ and $\chi_{hf}$, respectively) were measured using a Kappabridge MFK1-FA (AGICO). Frequency-dependent magnetic susceptibility ($\chi_{fd}$) was calculated from the expression $\chi_{fd}$ (%) $= [(\chi_{lf} - \chi_{hf})/\chi_{lf}] \times 100$. Variation of MS with temperature ($\kappa$–$T$ curves) was measured using CS4/CSL high- and low-temperature units attached to the

Kappabridge MFK1-FA. Anhysteretic remanent magnetization (ARM), expressed as susceptibility of ARM ($\chi_{ARM}$) in this paper, was imparted with an AF peak field of 100 mT and a DC biasing field of 0.1 mT using a 2G-755 magnetometer. Stepwise thermal demagnetization of triaxial isothermal remanent magnetization (IRM) (applied fields 1.0T, 0.3T, and 0.1T) and alternating field (AF) demagnetization were performed using a 2G-755 magnetometer. Hysteresis parameters, which are helpful to identify the type and particle size of magnetic minerals (Day et al. 1977; Dunlop 2002a, b; Zan et al. 2010), were measured using a MicroMag 2900, with a maximum applied field of 0.5 T. IRM acquisition curves were determined using a MMPM9 pulse magnetizer (maximum applied field 2.5 T) and a Molspin Minispin magnetometer. The contribution of different magnetic components was quantified using the IRMUNMIX2_2 and IRM_CLG1 routines to analyse cumulative log-Gaussian (CLG) IRM acquisition curves (Kruiver et al. 2001; Heslop et al. 2002; Gong et al. 2009).

## Results

### Thermal variation of magnetic susceptibility

Variation of MS with temperature ($\kappa$–$T$ curves) is widely used to identify the type of magnetic minerals (Evans and Heller 2003). Low- and high-temperature measurements are illustrated in Fig. 2 for surface sediments from all three cores (A8, A9, E601) and for samples from different depths (0–2, 8–10, 38–40 cm) within core E601.

Low-temperature $\kappa$–$T$ curves show a high paramagnetic contribution and a clear Verwey transition (Liu et al. 2010b) between −160 and −140 °C within cores A9 and A8, but not so obvious for E601, indicating the presence of magnetite. Samples from all cores and all depths display a very similar behavior in the heating curves. The $\kappa$ value dramatically increases after heating above 450 °C due to new formation of magnetite. A small decrease around 300 °C during heating suggests the existence of iron sulfides. A Curie temperature of magnetite in the heating curves in conjunction with a constant $\kappa$ value below 450 °C indicate that initial magnetite is existing in the surface samples of all cores. However, the relative increase of $\kappa$ in E601 is clearly higher than in A8 and A9, probably because of a lower initial content of magnetite.

### IRM acquisition and CLG analysis

Results of CLG analysis reveal a low-coercivity phase (likely representing magnetite) and a high-coercivity phase for all studied samples (Fig. 3). Contributions to IRM are ~77–89 and ~11–23 %, with $B_{1/2}$ varying between ~37–44 and ~216–769 mT for the soft and hard coercive components, respectively. The results indicate that the first component (magnetite) is the predominating magnetic mineral.

### Thermal and alternating field demagnetization of IRM

Thermal demagnetization (ThD) and alternating field demagnetization (AfD) of saturation IRM (SIRM) were performed to determine the type of the ferrimagnetic mineral indicated by the decay around 300°C in the $\kappa$–$T$ curves and by the higher coercivity component in the CLG analysis. A drop between 300 and 320 °C is also occurring during ThD of a triaxial SIRM (in particular, in the direction of highest acquisition field) and susceptibility measured after each step of ThD (Fig. 4a, b) indicating that iron sulfides are existing in the sediments (Roberts 1995; Sagnotti et al. 2005). A gyroremanent magnetization (GRM) is obvious above about 60 mT during AFD (Fig. 4c), which is a strong hint that greigite is present in the samples (Hu et al. 2002; Roberts et al. 2011).

## Discussion

The CLG analysis has demonstrated the presence of two components, from which the lower coercive one (component 1) represents magnetite while the harder coercive one (component 2) is likely related to greigite. The presence of greigite is mainly identified by GRM acquisition. Greigite is clearly contributing to magnetic remanence as evidenced by thermal demagnetization of the 1.0 T IRM. On the other hand thermal runs of MS show only a weak indication of greigite which can be explained by its high coercivity in these samples. The so far reported values for coercivity of greigite span a relatively wide range, but do not reach more than about 100 mT (Hoffmann 1992; Roberts 1995; Chang et al. 2007). However, Chang et al. (2008) investigated magnetic properties for pure synthetic greigite and found that it is not fully saturated even in a 5-T field. We therefore conclude that in these analyzed samples, MS is mainly controlled by the magnetite concentration while remanence parameters as ARM and (S)IRM are influenced by both the magnetite and the greigite concentrations.

The magnetic grain size can be characterized by the Day diagram (Day et al. 1977), i.e., using the saturation remanent magnetization to saturation magnetization ratio (Mrs/Ms) together with the remanent coercivity to coercivity ratio (Hcr/Hc). Values of Mrs/Ms and Hcr/Hc are between 0.15–0.21 and 1.91–2.05, respectively, indicating that the magnetic domain state of the grains in these sediments is in the pseudo-single-domain range (Evans and Heller 2003; Dekkers 2007). However, the Day diagram is strictly only

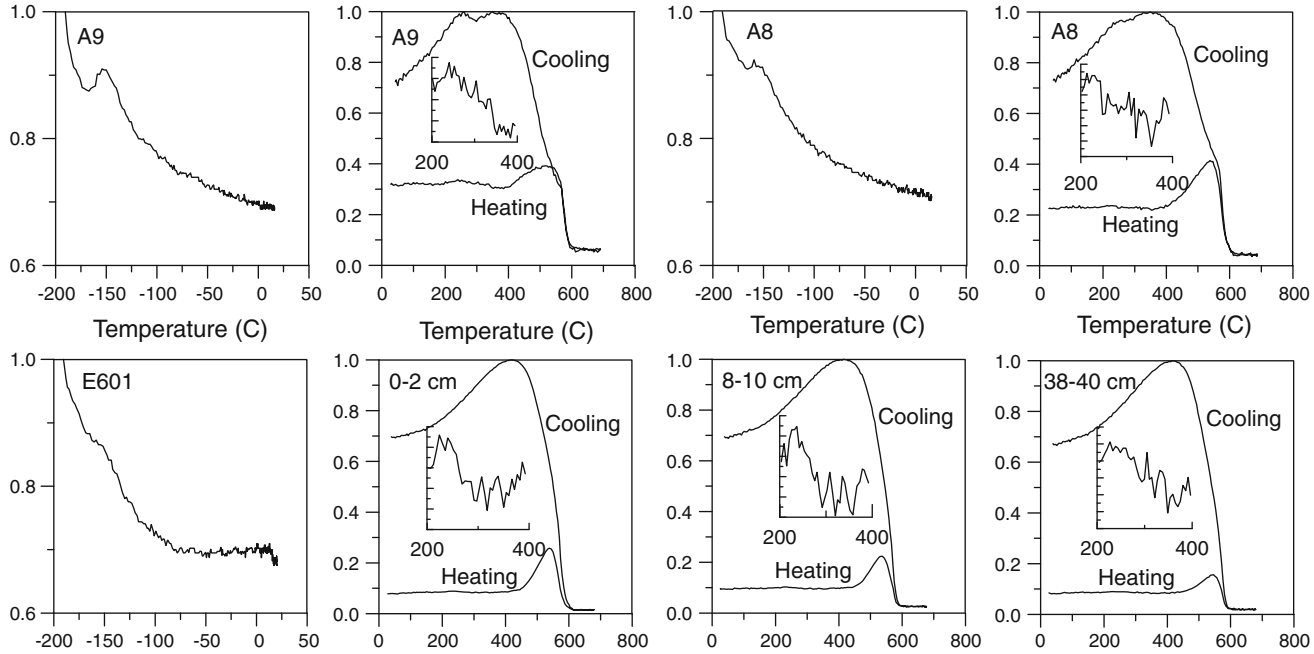


**Fig. 2** $\kappa$–$T$ curves for surface sediments (0–2 cm) from all three cores and for samples from different depths (0–2, 8–10, and 38–40 cm) of core E601. *Small inserted figures* show enlargements of heating curves in the temperature interval 200–400 °C

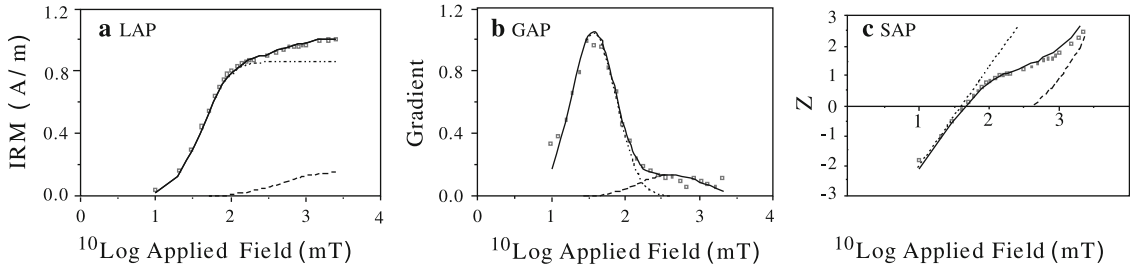


**Fig. 3** **a** LAP for a sediment sample mixture of component 1 (average contribution ~82 %, average $B_{1/2}$ ~39 mT) and component 2 (average contribution ~18 %, average $B_{1/2}$ ~414 mT). *Squares* represent input data. *Short- and long-dashed lines* represent component 1 and component 2, respectively. *Solid lines* represent the sum of the components. **b** GAP analysis for the sediment sample. Lines and symbols as in panel a. **c** SAP analysis for the sediment sample. Lines and symbols as in panel a

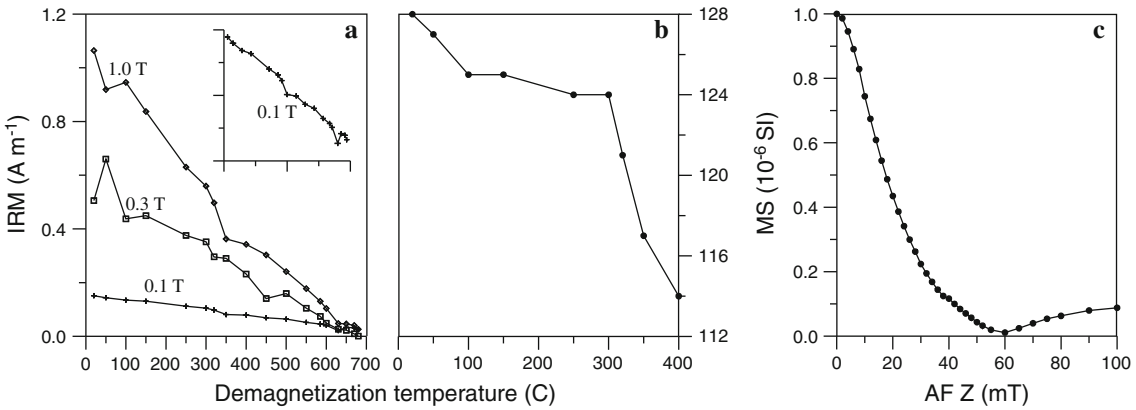


**Fig. 4** Triaxial IRM (applied fields to three orthogonal axes 1.0 T, 0.3 T, and 0.1 T) (**a**) and MS (**b**) measured at room temperature after thermal demagnetization from 50 to 700 and 400 °C, respectively, and (**c**) AF demagnetization (of an IRM acquired at a field 100 mT) showing gyromagnetic remanence acquisition at AF fields >60 mT

valid for magnetite, and the greigite content may distort the interpretation of hysteresis parameters (Chang et al. 2008; Roberts et al. 2011). Frequency-dependent MS ($\chi_{fd}$) indicates the relative contribution of superparamagnetic (SP) particles (Thompson and Oldfield 1986). Figure 5 shows a positive correlation of $\chi_{lf}$ with $\chi_{fd}$ (%) and $\chi_{ARM}$. From this result, it can be inferred that fine-grained (SD and SP) particles of magnetite (and possibly also greigite) play a more important role for samples with a higher total ferrimagnetic content. A significant positive correlation found between GRM intensity and ARM (Fig. 6) indicates that greigite is enhanced when the total concentration of ferrimagnetic constituents is higher. Furthermore, higher contribution of component 2 (higher coercivity phase) corresponds to higher low-frequency mass-specific MS ($\chi_{lf}$) (Fig. 6), indicating that for larger ferrimagnetic contents the second component (greigite) is more enhanced than the first (magnetite) one.

Contributions of the second component appear to have an increasing trend from E601, A8, to A9 (Fig. 6), which seems to be related to the distance between the core location (i.e., sedimentation area) and the material sources around the PRE Though $\chi_{lf}$ of sediments from core E601 is lower than for cores A8 and A9, $\chi_{fd}$ (%) for core E601 reaches the same values as cores A8 and A9. The role of water transport may explain this result. Compared to A8 and A9, core E601 receives a lower portion of ferrimagnetic particles in total, but smaller ferrimagnetic grains from the PRD may be transported through a longer distance.

Magnetic enhancement of both magnetite and greigite is likely related to environmental pollution of the surrounding areas. Many previous studies suggested that iron sulfides are of importance in polluted environments (Dekkers and Schoonen 1994; Cornwell and Morse 1987; Snowball and Torii 1999; Power and Worsley 2009). As discussed above, greigite is existing within the coastal sediments and its concentration is mainly appearing in magnetic remanence parameters (ARM and SIRM) while in the magnetic susceptibility signal magnetite is clearly dominating. Although variation of magnetic parameters is not completely consistent for the three cores, three stages related to well-known development phases in China can be identified from the vertical variation of the magnetic parameters illustrated in Fig. 7. Phase A recorded by cores A9 and A8 with an increase of concentration parameters $\chi$, SIRM, and ARM is related to the iron smelting phase in China mainland together with labor-intensive manufacturing activities in Hong Kong from 1950s to early 1960s. Iron phases and sulfur, one of the fossil fuel combustion products, can deposit directly or indirectly into coastal waters. Magnetite and different iron sulfides, including greigite, can form through a series of chemical and microbially mediated reactions within a reductive environment as coastal brackish water (Canfield 1989). An obvious decrease in ferrimagnetic concentration recorded by core A8 (phase B in Fig. 7) can be explained by a decrease of iron phases and sulfur discharge due to the cultural revolution in China mainland after mid-1960s when industrial development was nearly stopped (Clark 2008).

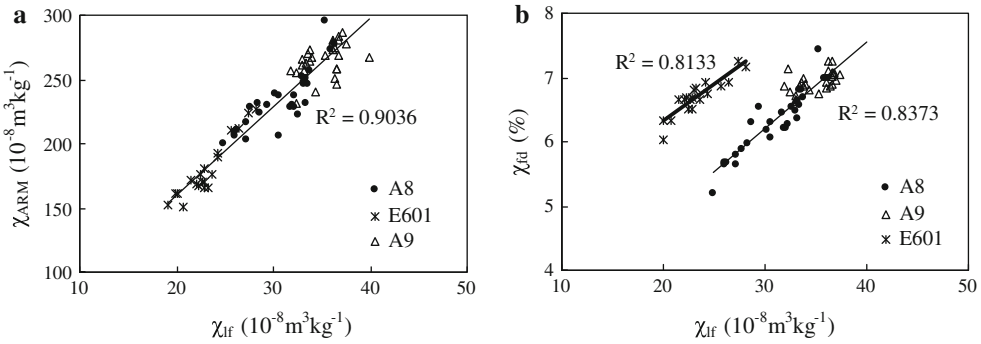


**Fig. 5** Relationship between (low frequency) mass specific MS and **a** $\chi_{ARM}$, **b** $\chi_{fd}$ (%)

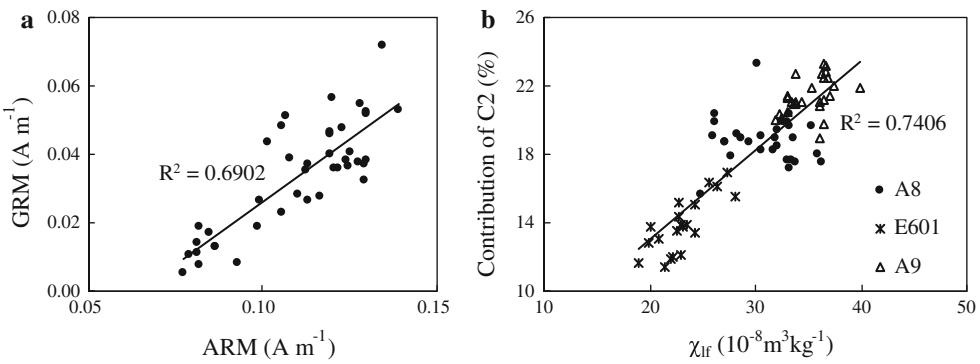


**Fig. 6** Correlationship between **a** GRM and ARM, **b** $\chi_{lf}$ and the contribution of the second component (C2)

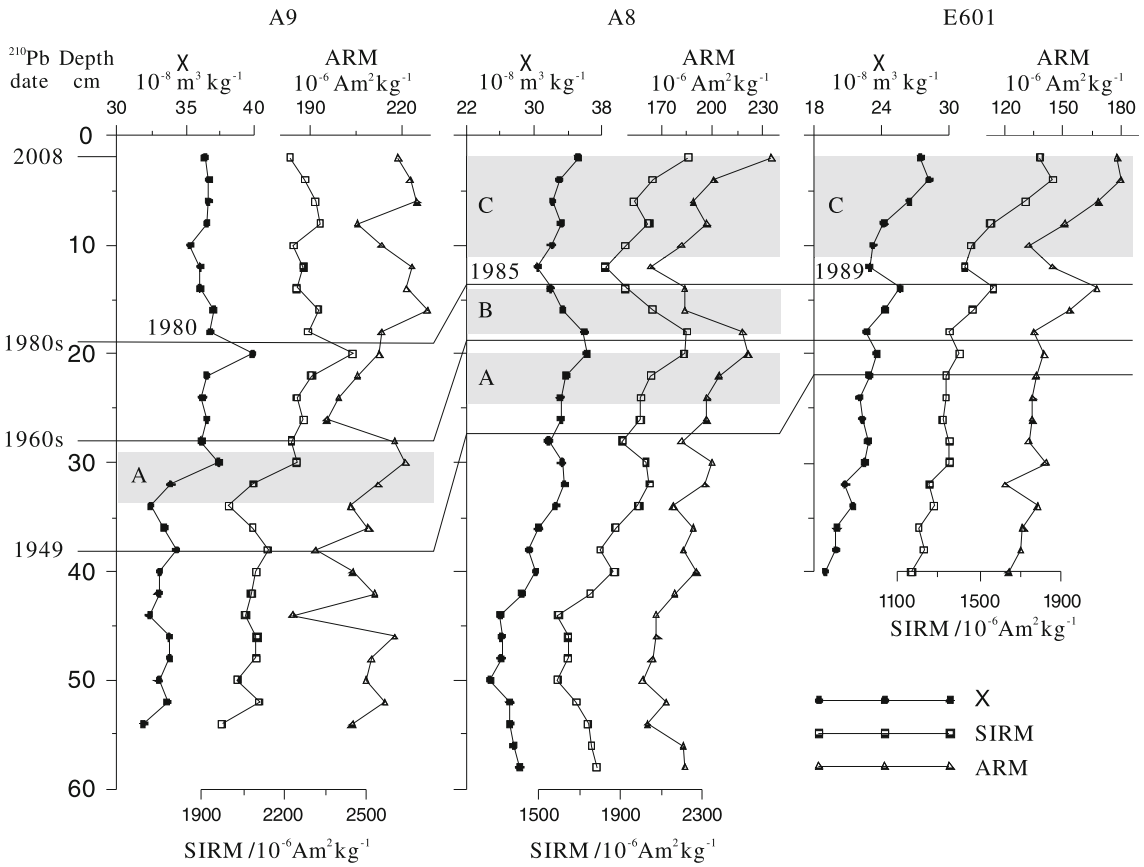


**Fig. 7** Vertical variation of MS, ARM, and SIRM with corresponding $^{210}$Pb dates (*numbers on phased lines* are $^{210}$Pb dates) for the three cores

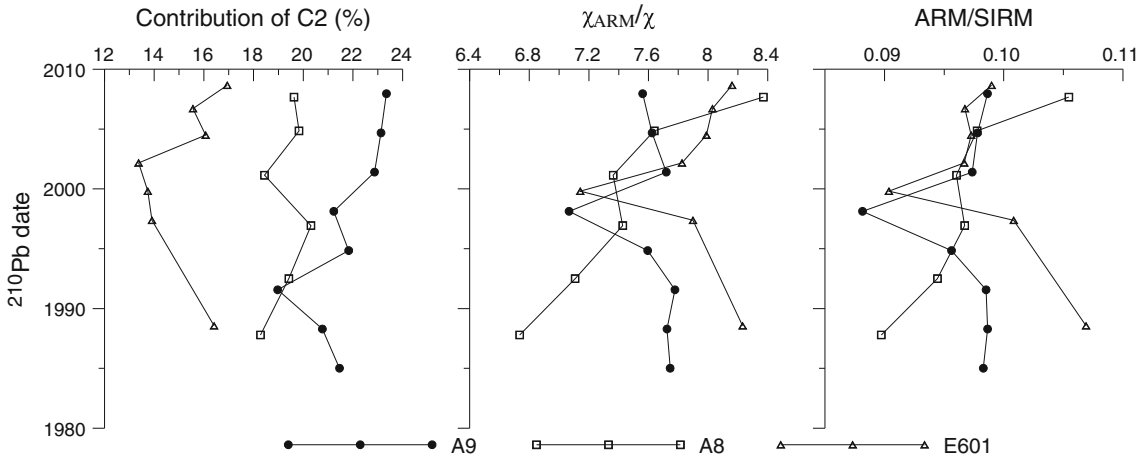


**Fig. 8** Variation of contribution of component 2, $\chi_{ARM}/\chi$, and ARM/SIRM since 1980s for all cores

Industrialization has been promoted since the "open door" policy was implemented from late 1970s, especially after the PRD was designated as an Economic Zone by the State Council of People's Government of China in 1985. More and more iron phases and sulfur were discharged from recently established factories related to industries such as electronics, apparel, cement, etc. (Sung et al. 1996). As a result, concentration-dependent magnetic parameters $\chi$, SIRM, and ARM increased continuously during the last decade (pointed out as phase C in Fig. 7). Despite values of magnetic concentration parameters are higher in A9 than A8 and E601, a slight decrease instead of an increase appear s in core A9 during this period. As many previous research suggested (Berner et al. 1979; Cutter and Velinsky 1988;

Torii et al. 1996; Sternbeck and Sohlenius 1997), magnetite can transform to iron sulfides within the reductive environment of coastal waters. Compared to A8 and E601, contribution of component 2 (greigite) reached a relatively high level in sediments of core A9 (Fig. 8a). More greigite and less magnetite may be one reason for the 'missing decrease and increase' of concentration parameters in core A9 after 1960 (Hu et al. 2002; 2003). However, the threshold of the ratio between greigite and magnetite for MS reduction remains unknown. Unlike core A8, magnetic granulometry parameters, $\chi_{ARM}/\chi$ and ARM/SIRM, which are sensitive to SD particles (Thompson and Oldfield 1986; Egli and Lowrie 2002) show a decreasing trend since 1980s for core A9 (Fig. 8b, c) indicating that relative concentration of SD particles decreased.

## Conclusion

Main magnetic minerals in the sediments from South China coastal waters are magnetite and probably some high-coercivity greigite; greigite is more enhanced than magnetite when the total concentration of magnetic minerals is higher. In such samples with increased ferromagnetic content fine-grained (SP and SD) ferrimagnetic particles play a more important role.

Three stages corresponding to specific well-know events in China were identified from the vertical variation of magnetic parameters. The iron-smelting phase and the opening and reforming phases in China are expressed by increasing values of magnetic susceptibility and magnetic remanences. A decreasing trend of these concentration parameters was observed during the cultural revolution when industrial development almost stopped. Core A9 does not reflect the trends after 1960. The reason may be an increasing content of greigite on expense of SD magnetite due to a reductive environment (Hu et al. 2001; Yue and Huang 2005). Though more work has to be done to study a denser net of cores, it can be optimistic that magnetic concentration parameters in coastal sediments can reflect the development history in the Pearl River delta.

**Acknowledgments** This research was partially funded by the National Basic Research Project (2009CB421206, 2010CB833405) and "Tu Guangchi" Talents Fund of Guangzhou Institute of Geochemistry, CAS (GIG-08-0301). Authors would like to thank Weifang Chen for providing the $^{210}$Pb dates. Thanks are also extended to Weilin Zhang for assistance with magnetic measurements.

## References

Alagarsamy R (2009) Environmental magnetism and application in the continental shelf sediments of India. Marine Environ Res 68:49–58

Berner RA, Baldwin T, Holdren GR (1979) Authigenic iron sulfides as paleosalinity indicators. J Sediment Res 49:1345–1350

Bityukova L, Scholger R, Birke M (1999) Magnetic susceptibility as indicator of environmental pollution of soils in Tallinn. Phys Chem Earth A 24:829–835

Canfield DE (1989) Reactive iron in marine sediments. Geochim Cosmochim Acta 53:619–632

Chang L, Roberts AP, Muxworthy AR, Tang Y, Chen QW, Rowan CJ, Liu QS, Pruner P (2007) Magnetic characteristics of synthetic pseudo-single-domain and multi-domain greigite ($Fe_3S_4$). Geophys Res Lett doi:10.1029/2007GL032114

Chang L, Roberts AP, Tang Y, Rainford BD, Muxworthy AR, Chen QW (2008) Fundamental magnetic parameters from pure synthetic greigite ($Fe_3S_4$). J Geophys Res doi:10.1029/2007JB005502

Clark P (2008) The Chinese cultural revolution: a history. Cambridge university press, New York

Cornwell J, Morse J (1987) The characterization of iron sulfide minerals in anoxic marine sediments. Mar Chem 22:193–206

Cutter GA, Velinsky DJ (1988) Temporal variations of sedimentary sulfur in a Delaware salt marsh. Mar Chem 23:311–327

Day R, Fuller MD, Schmidt VA (1977) Hysteresis properties of titanomagnetites: grain size and composition dependent. Phys Earth Planet Int 13:260–266

Dekkers MJ (2007) Magnetic proxy parameters. In: Gubbins D, Herrero-Bervera E (eds) Encyclopedia of geomagnetism and paleomagnetism. Springer, Dordrecht, pp 525–534

Dekkers MJ, Schoonen AA (1994) An electrokinetic study of synthetic greigite and pyrrhotite. Geochim Cosmochim Acta 58:4147–4153

Dunlop DJ (2002a) Theory and application of the Day plot (Mrs/Ms versus Hcr/Hc) 1: theoretical curves and tests using titanomagnetite data. J Geophys Res. doi:10.1029/2001JB000486

Dunlop DJ (2002b) Theory and application of the Day plot (Mrs/Ms versus Hcr/Hc) 2: application to data for rocks, sediments and soils. J Geophys Res. doi:10.1029/2001JB000487

Egli R, Lowrie W (2002) Anhysteretic remanent magnetization of fine magnetic particles. J Geophys Res. doi:10.1029/2001JB000671

Evans ME, Heller F (2003) Environmental magnetism: principles and applications of enviromagnetics. Academic Press, San Diego

Evans ME, Heller F, Bloemendal J, Thouveny N (1997) Natural magnetic archives of past global change. Surv Geophys 18:183–196

Garming JFL (2006) Diagenetic imprints on magnetic mineral assemblages in marine sediments: unpublished PhD thesis. University Bremen, Germany

Gautam P, Blaha U, Appel E, Neupane G (2004) Environmental magnetic approach towards the quantificaton of pollution in Kathmandu urban area, Nepal. Phys Chem Earth 29:973–984

Ghilardi M, Kunesch S, Styllas M, Fouache E (2008) Reconstruction of Mid-Holocene sedimentary environments in the central part of the Thessaloniki Plain (Greece), based on microfaunal identification, magnetic susceptibility and grain-size analyses. Geomorphology 97:617–630

Gong Z, Dekkers MJ, Heslop D, Mullender AT (2009) End-member modelling of isothermal remanent magnetization (IRM) acquisition curves: a novel approach to diagnose remagnetization. Geophys J Int. doi:10.1111/j.1365-246X.2009.04220.x

Heslop D, Dekkers MJ, Kruiver PP, Oorschot IHM (2002) Analysis of isothermal remanent magnetization acquisition curves using the expectation-maximization algorithm. Geophys J Int 148:58–64

Hilton J (1987) A simple model for the interpretation of magnetic records in lacustrine and ocean sediments. Quat Res 27:160–166

Hoffmann V (1992) Greigite ($Fe_3S_4$): magnetic properties and first domain observations. Phys Earth Planet Int 70:288–301

Horng CS, Chen KH (2006) Complicated magnetic mineral assemblages in marine sediments offshore of Southwestern Taiwan: possible influence of methane flux on the early diagenetic process. Terr Atmospheric Ocean Sci 17:1009–1026

Hu CY, Pan JM, Liu XY (2001) Species of phosphorus in sediments from Pearl River Estuary. Marine Environ Sci 20(4):21–25 (In Chinese with English abstract)

Hu SY, Appel E, Hoffmann V, Schmahl W (2002) Identification of greigite in lake sediments and its magnetic significance. Sci China Ser D 45:81–87

Hu SY, Wang Y, Appel E, Zhu Y, Hoffmann V, Shi C, Yu Y (2003) Magnetic responses to acidification in lake Yangzonghai, SW China. Phys Chem Earth 28:711–717

Huh CA, Su CC, Wang CH, Lee SY, Lin IT (2006) Sedimentation in the southern Okinawa trough: rates, turbidities and a sediment budget. Mar Geol 231:129–139

Jordanova D, Veneva L, Hoffmann V (2003) Magnetic susceptibility screening of anthropogenic impact on the Danube river sediments in Northwestern Bulgaria-preliminary results. Stud Geophys Geod 47:403–418

Krishnaswami S, Lal D, Martin JM, Meybeck M (1971) Geochronology of lake sediments. Earth Planet Sci Lett 11:407–414

Kruiver PP, Dekkers MJ, Heslop D (2001) Quantification of magnetic coercivity components by the analysis of acquisition curves of isothermal remanent magnetisation. Earth Planet Sci Lett 189:269–276

Kumar AA, Rao VP, Patil SK, Kessarkar PM, Thamban M (2005) Rock magnetic records of the sediments of the eastern Arabian Sea: evidence for late quaternary climatic change. Mar Geol 220:59–82

Li ZG, Chu FY, Zhang FY, Chen L, Zhang H (2011) Distribution pattern of heavy minerals in the surface sediments on inner shelf, northwest South China Sea and its controlling factors. Marine Geol Quat Geol 31(4):89–96 (In Chinese with English abstract)

Lin CS (1997) Red capitalism in South China: growth and development of the Pearl River Delta. UBC Press, Vancouver

Liu JG, Chen Z, Chen MH, Yan W, Xiang R, Tang XZ (2010a) Magnetic susceptibility variations and provenance of surface sediments in the South China Sea. Sed Geol 230:77–85

Liu XM, Shaw J, Jiang JZ, Bloemendal J, Hesse P, Rolph T, Mao XG (2010b) Analysis on variety and characteristics of maghemite. Sci China Earth Sci 53:1153–1162

Lo CP (1989) Recent spatial restructuring in Zhujiang Delta, South China: a study of socialist regional development strategy. Ann Assoc Am Geogr 79:293–308

Locke G, Bertine KK (1986) Magnetite in sediments as an indicator of coal combustion. Appl Geochem 1:345–356

Lu SG, Bai SQ, Xue QF (2007) Magnetic properties as indicators of heavy metal pollution in urban topsoils: a case study from the city of Luoyang, China. Geophys J Int 171:568–580

Maher BA (2007) Environmental magnetism and climate change. Contemp Phys 48:247–274

Martins CC, Mahiques MM, Bícego MC, Fukumoto MM, Montone RC (2007) Comparison between anthropogenic hydrocarbons and magnetic susceptibility in sediment cores from the Santos Estuary, Brazil. Mar Pollut Bull 54:226–246

Meena NK, Maiti S, Shrivastava A (2011) Discrimination between anthropogenic (pollution) and lithogenic magnetic fraction in urban soils (Delhi, India) using environmental magnetism. J Appl Geophys 73:121–129

Nittrouer CA, Sternberg RW, Carpenter R, Bennett JT (1979) The use of Pb-210 geochronology as a sedimentological tool: application to the Washington continental shelf. Marine Geology 31:297–316

Plater AJ, Appleby PG (2004) Tidal sedimentation in the Tees estuary during the 20th century: radionuclide and magnetic evidence of pollution and sedimentary response. Estuar Coast Shelf Sci 60:179–192

Plater AJ, Ridgway J, Appleby PG, Berry A, Wright MR (1998) Historical contaminant fluxes in the Tees estuary, UK: geochemical, magnetic and radionuclide evidence. Mar Pollut Bull 37:343–360

Power AL, Worsley AT (2009) Using urban man-made ponds to reconstruct a 150-year history of air pollution in northwest England. Environ Geochem Health 31:327–338

Ridgway J, Shimmield G (2002) Estuaries as repositories of historical contamination and their on shelf seas. Estuar Coast Shelf Sci 55:903–928

Roberts AP (1995) Magnetic properties of sedimentary greigite ($Fe_3S_4$). Earth Planet Sci Lett 134:227–236

Roberts AP, Chang L, Rowan CJ, Horng CS, Florindo F (2011) Magnetic properties of sedimentary greigite ($Fe_3S_4$): an update. Rev Geophys. doi:10.1029/2010RG000336

Sagnotti L, Roberts AP, Weaver R, Verosub KL, Florindo F, Pike CR, Clayton T, Wilson GS (2005) Apparent magnetic polarity reversals due to remagnetization resulting from late diagenetic growth of greigite from siderite. Geophys J Int 160:89–100

Sangode SJ, Sinha R, Phartiyal B, Chauhan OS, Mazari RK, Bagati TN, Suresh N, Mishra S, Kumar R, Bhattacharjee P (2007) Environmental magnetic studies on some Quaternary sediments of varied depositional settings in the Indian sub-continent. Quat Int 159:102–118

Snowball I, Torii M (1999) Incidence and significance of magnetic iron sulphides in Quaternary sediments and soil. In: Maher BA, Thompson R (eds) Quaternary Climates, environments and magnetism. University Press, Cambridge, pp 199–230

Sternbeck J, Sohlenius G (1997) Authigenic sulfide and carbonate mineral formation in Holocene sediments of the Baltic Sea. Chem Geol 135:55–73

Sung YW, Liu PW, Wong YCR, Lau PK (1996) The fifth dragon: the emergence of the Pearl River Delta. Addison-Wesley Pub Co Press, Reading

Thompson R, Oldfield F (1986) Environmental magnetism. George Allen and Unwin, London

Torii M, Fukuma K, Horng CS, Lee TQ (1996) Magnetic discrimination of pyrrhotite- and greigite-bearing sediment samples. Geophys Res Lett 23:1813–1816

Wang YH, Yu ZG, Li GX, Oguchi T, He HJ, Shen HT (2009) Discrimination in magnetic properties of different-sized sediments from the Changjiang and Huanghe estuaries of China and its implication for provenance of sediment on the shelf. Marine Geol 260:121–129

Yang XQ, Rodney G, Zhou HY, Yang J (2008) Magnetic properties of sediments from the Pearl River Delta, South China: paleoenvironmental implications. Sci China Earth Sci. doi: CNKI:SUN:JDXG.0.2008-01-007

Yim WWS, Huang G, Chan LS (2004) Magnetic susceptibility study of late quaternary inner continenta shelf sediments in the Hong Kong SAR, China. Quat Int 117:41–54

Yu LZ, Oldfield F (1989) A multivariate mixing model for identifying sediment source from magnetic measurements. Quat Res 32:168–181

Yue WZ, Huang XP (2005) Distribution characteristics of phosphorus in core sediments from Zhujiang River Estuary and its environmental significance. J Trop Oceanogr 24(1):21–27 (In Chinese with English abstract)

Zan JB, Fang XM, Yang SL, Nie JS, Li XY (2010) A rock magnetic study of loess from the West Kunlun mountains. J Geophys Res. doi:10.1029/2009JB007184

Zhang WG, Yu LZ, Hutchinson SM (2001) Diagenesis of magnetic minerals in the intertidal sediments of the Yangtze Estuary,

China, and its environmental significance. Sci Total Environ 266:169–175

Zhang L, Chen FR, Ying KD, Lv Y, Yang YQ, Zhang DR (2010) The characteristics and sources of surface sediments in the Pearl River Estuary and its adjacent shelves. J Trop Oceanogr 29(1):98–103 (In Chinese with English abstract)

Zheng Y, Kissel C, Zheng HB, Laj C, Wang K (2010) Sedimentation on the inner shelf of the East China Sea: magnetic properties, diagenesis and paleoclimate implications. Mar Geol 268:34–42